Dynamic self-assembly of a double hydrophilic block glycopolymer

Oh, Takahiro
Department of Chemical Engineering, Kyushu University

Hoshino, Yu
Department of Chemical Systems and Engineering, Kyushu University

Miura, Yoshiko
Department of Chemical Systems and Engineering, Kyushu University

出版情報：Journal of materials chemistry B. 44, pp.10101-10107, 2020-10-16. Royal Society of Chemistry
バージョン：
権利関係：

ARTICLE

Dynamic self-assembly of a double hydrophilic block glycopolymer

Received 00th January 20xx,
Accepted 00th January 20xx

DOI: 10.1039/x0xx00000x

Takahiro Oh, [a] Yu Hoshino [a] and Yoshiko Miura *[a]

Double hydrophilic block glycopolymers (DHBGs) composed of glycopolymers and polyethylene glycol (PEG) self-assemble in aqueous solution. However, there are no guidelines to direct and design DHBG self-assembly. Herein, we investigated the effect of the ratio of glycopolymer length to PEG length on the self-assembled structure, and report that structure size could be influenced by the block polymer ratio. Nine kinds of DHBG with different glycopolymers and PEG lengths were synthesized via reversible addition–fragmentation chain transfer (RAFT) polymerization. The self-assembly capability of DHBG was investigated by transmission electron microscopy (TEM) and dynamic light scattering (DLS). In all cases, the DHBGs self-assembled into the spherical structures, even when the PEG and glycopolymer lengths were quite different. The size of the self-assembled structure was controlled by the ratio of the PEG length to the glycopolymer length. The self-assembly of the DHBGs was induced by hydrogen bonding between the sugar moieties. The dynamic self-assembly of the DHBG was affected by temperature and concentration.

1. Introduction

Self-assembly is one of the most fundamental characteristics of life. All living cells have membranes comprising self-assembled lipids that create well-ordered, isolated compartments, thereby promoting specific interactions and chemical reactions.[1] Various substrates are localized by compartmentalization, which enables the precise regulation of hundreds of chemical processes.

Compartmentalization is applicable to the chemical sciences as well as to biology. Self-assembled structures create micro-spaces with a variety of applications such as drug delivery system and nano reactor.[2] The self-assembly of amphiphilic block copolymers inspired by lipid membranes has been studied for many decades.[3–5] However, lipid membranes rely on hydrophobicity, which limit the mass transfer of water-soluble substrate between inside and outside of nano reactor.[6] Synthetic self-assembled structures with no hydrophobic barrier are therefore highly desirable.

In recent years, self-assembly that does not rely on hydrophobic interactions has begun to attract attention.[7–14] Some polysaccharides—such as pullulan with polyethylene glycol (PEG) or other hydrophilic polymer—are water-soluble but do not readily mix with water, and are prone to phase separation.[9,15,16] This phenomenon promotes the self-assembly of pullulan–PEG block polymers in water. On the other hand, there are some reports about self-assembly of hydrophilic block copolymer using electrostatic interaction[12,13,17] or a coordination bond with metal ion[7,8] as a driving force. There are still only a few examples of the self-assembly of water-soluble polymers by hydrogen bonds, especially in water. Previously, we reported the self-assembly of a double hydrophilic block glycopolymer (DHBG) driven by hydrogen bonding and coordination to calcium ions in water.[18] The DHBG comprised PEG and a glycopolymer with a high-density mannose (monosaccharide) side chain. This is a novel self-assembly using glycopolymer, which are usually used as water-soluble groups[19], as a driving force for self-assembly.

Such DHBGs self-assemble in water via a different mechanism to amphiphilic block copolymers, and consequently may have different properties. DHBGs lack a hydrophobic barrier, and the water phase exists in their interiors instead. In other words, these synthetic polymers create a special aqueous micro-space isolated from the rest of the water phase. Such compartmentalization by synthetic polymers may also be capable of localizing and concentrating various water-soluble substances in aqueous solution with less limitation of transportation.

Amphiphilic block copolymers self-assemble into various structures such as micelles, worms, and vesicles based on the packing parameter model.[4] However, in the case of DHBG, it is unclear how the ratio of each block polymer affects the morphology of self-assembly. Unlike an amphiphilic block copolymer, DHBG comprises two kinds of hydrophilic polymers. The self-assembly of DHBG occurs via molecular interactions such as hydrogen bonding in the sugar moieties, so the mechanism of self-assembly is totally different to that found in amphiphilic block copolymers. In the present study, we investigated the effect of the ratio of glycopolymer to PEG length (M_{DP}/P_{DP}) on the self-assembly of structures to create a

[a] *Department of Chemical Engineering, Kyushu University, 744 Motooka, Nishiku, Fukuoka 819-0395, Japan.*

Electronic Supplementary Information (ESI) available: [details of any supplementary information available should be included here]. See DOI: 10.1039/x0xx00000x

guideline for DHBG self-assembly. We have developed a readily controlled method of synthesizing a DHBG comprising a glycopolymer with a mannose side chain and a PEG block, using reversible addition–fragmentation chain transfer (RAFT) polymerization. Nine DHBG variants with different glycopolymer and PEG lengths were synthesized to investigate the correlation between the block ratio and self-assembly. The self-assembled structure of each DHBG was investigated by transmission electron microscopy (TEM) and dynamic light scattering (DLS). The dynamic properties of the DHBG were also investigated by changing the temperature and polymer concentration.

2. Experimental section

2-1. Material

2,2′-Azobisisobutyronitrile (AIBN) (98%), calcium chloride (95%), and 2-[4-(2-hydroxyethyl)piperazin-1-yl]ethanesulfonic acid (HEPES) (99%) were purchased from FUJIFILM Wako Pure Chemical Corporation. Osmium tetroxide (4% in water) and polyethylene glycol monomethyl ether (Mw: 400, 2000, and 4000) were purchased from Tokyo Chemical Industry. Sodium chloride (99%), magnesium chloride hexahydrate (99%), potassium chloride (99.5%), and dry *N*,*N*-dimethylformamide (DMF) (99.5%) were purchased from Kanto Chemical. Dimethyl sulfoxide (DMSO, 98%) was purchased from Kishida.

2-2. Characterization

^{1}H NMR spectra were recorded on a JNM-ECZ400 spectrometer (JEOL, Tokyo, Japan) using $CDCl_3$, d_6-DMSO, or D_2O as a solvent. Gel permeation chromatography (GPC) with organic solvent was performed on a HLC-8320 GPC Eco-SEC system equipped with a TSKgel Super AW guard column and TSKgel Super AW (4000, 3000, and 2500) columns (Tosoh, Tokyo, Japan). GPC with water solvent was performed on a JASCO DG-980-50 degasser equipped with a JASCO PU-980 pump (JASCO Co., Tokyo, Japan), a Shodex OHpak SB-G guard column, a Shodex OHpak LB-806 HQ column (Showa Denko, Tokyo, Japan), a JASCO RI-2031 Plus RI detector. GPC analyses were performed by injecting 20 μL of a polymer solution (1 g L^{-1}) in DMF buffer containing LiBr (10 mM) or $NaNO_3$ aqueous solution (100 mM). The buffer solution was also used as the eluent at a flow rate of 0.5 mL min^{-1}. The GPC system was calibrated using a poly(methyl methacrylate) standard(Shodex) for organic solvent GPC and pullulan standard (Shodex) for aqueous GPC.

2-3. General procedure for RAFT polymerization

The syntheses of (d-mannose-1*H*-1,2,3-triazol-4-yl) methyl methacrylate (Man-MA), poly (ethylene glycol) 4-(((butylthio)carbonothioyl)thio)-4-cyanopentanoate (PEG-CTA) and 4-(((butylthio)carbonothioyl)thio)-4-cyanopentanoic acid are described in the Supporting Information. Man-MA was introduced to a glass tube and mixed with a DMSO solution of PEG-CTA or 4-(((butylthio)carbonothioyl)thio)-4-cyanopentanoic acid as the RAFT agent and AIBN as the radical initiator. The [Man-MA] : [RAFT agent] : [initiator] ratios are shown in Table 1. The tube was degassed with freeze–pump–thaw cycles, sealed under vacuum, and transferred to an oil bath at 60°C. After heating for 15 h, polymerization was stopped by cooling the solution with liquid nitrogen. Subsequently, the polymer solutions were dialyzed against DMSO (three times) and water (three times). The resultant polymer solution was then freeze-dried. The polymer, which has unreacted PEG confirmed by GPC, were washed by toluene to remove unreacted PEG. The conversion and degree of polymerization were determined by ^{1}H NMR (Table 2). The polydispersity of the polymer was determined by GPC (Table 2).

2-4 Turbidity measurement by UV-Vis spectrometer

Mannose homopolymer ($\mathbf{M_{200}}$) was dissolved in HEPES buffer containing NaCl or guanidium hydrochloride (4 M), and incubated for 23 h at 5°C. The ultraviolet–visible (UV-Vis) spectra were recorded on an Agilent 8453 spectrometer (Agilent Technologies Inc., Santa Clara, CA, USA).

2-5. Dynamic light scattering (DLS) measurement

The DLS measurements were obtained using a ZETASIZER NANO-ZS system (Malvern, UK). Particle sizes were measured at 5°C in HEPES buffer (HEPES, 10 mM; NaCl, 136.9 mM; KCl, 2.68 mM; $CaCl_2$, 1.80 mM; $MgCl_2 \cdot 6H_2O$, 0.49 mM) at polymer concentrations of 1 g L^{-1} and 10 g L^{-1} after incubation at 5°C for 16 h. Owing to low dispersibility, the incubation time of P_9M_{200} (1 g L^{-1}) was 5 h. The DLS measurements were obtained at least three times to confirm the reproducibility. For temperature-swing DLS measurement, the hydrodynamic diameter, was measured every 2 mins at increments of 5°C as the temperature was gradually decreased from 40 to 5°C, and then gradually increased from 5 to 40°C. The scattering of large particles was larger than that of small particles, which greatly influenced the intensity distribution. Therefore, approximate volume distribution was thus evaluated.

2-6. Transmission electron microscope (TEM) observation

TEM images of each DHBG were obtained using an FEI TECNAI-20 system (Thermo). Each DHBG was dissolved in HEPES buffer (HEPES, 10 mM; NaCl, 136.9 mM; KCl, 2.68 mM; $CaCl_2$, 1.80 mM; $MgCl_2 \cdot 6H_2O$, 0.49 mM). The TEM grid was hydrophilized by plasma treatment for 30 s, and then 2 μL of each polymer solution was dropped onto the grid. The grid was incubated for 1 min at 5°C, and excess solution was removed with paper. Osmium tetroxide solution was then dropped onto the TEM grid, which was incubated for 30 s at 5°C. Excess solution was again removed with paper and the TEM images were obtained at 120 kV.

3. Result and discussion

3-1. Synthesis of double hydrophilic block glycopolymer

The DHBGs (PEG_m-poly(mannose)$_n$, denoted as $\mathbf{P_mM_n}$ (m = 9, 45, and 90; n = 10, 100, and 200), were synthesized as shown in Scheme 1. DHBGs with different PEG and glycopolymer lengths were obtained by RAFT polymerization with Man-MA and PEG-CTA. The feed ratios (**m**) of [Man-MA]/[RAFT agent] were 10, 100, and 200, as described in Table 1 and 2. In addition, the degree of polymerization values of ethylene glycol in PEG-CTA (**n**) were 9, 45, and 90. The monomer conversion values, which were calculated by ^{1}H NMR, were over 90% in all cases, and the

Scheme 1 RAFT polymerization of Man-MA

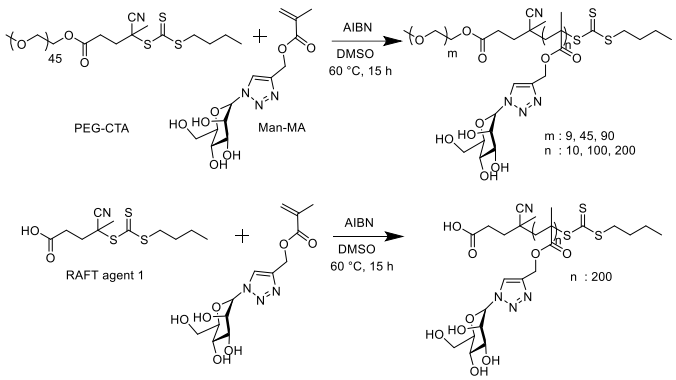

Table 1 The feed ratio of polymerization of Man-MA with PEG-CTA.

	Man-MA (mmol)	RAFT (mmol)	AIBN (mmol)	DMSO (mL)
P_mM_{10}	3.0×10^{-1}	3.0×10^{-2}	6.0×10^{-3}	0.5
P_mM_{100}	3.0×10^{-1}	3.0×10^{-3}	6.0×10^{-4}	0.5
P_mM_{200}	3.0×10^{-1}	1.5×10^{-3}	3.0×10^{-4}	0.5
M_{200}	3.0×10^{-1}	1.0×10^{-3}	3.0×10^{-3}	0.5

Table 2 The result of polymerization.

	Conv. (%)	DP (NMR)	M_n (NMR)	M_n (GPC)	PDI
P_9M_{10}	97.0	10	4000	5300	1.44
P_9M_{100}	97.3	101	33900	31200	1.48
P_9M_{200}	96.5	190	63200	61400	1.48
$P_{45}M_{10}$	95.8	15	7200	8900	1.27
$P_{45}M_{100}$	93.9	109	38100	52600	1.60
$P_{45}M_{200}$	83.0	192	65500	117900**	1.16**
$P_{90}M_{10}$	99.0	14	8900	13700	1.21
$P_{90}M_{100}$	97.5	90	33900	37900	1.47
$P_{90}M_{200}$	95.7	194	68100	56000	1.34
M_{200}	90.3	180*	59500	41700	1.46

*The DP was calculated from monomer conversion.

**The GPC measurement was carried out using $NaNO_3$ aqueous solution (100 mM).

degree of polymerization (DP) values of Man-MA (**n**) were as designed (Table 2). The polydispersity index (PDI) range of each DHBG, as determined by GPC analysis, was relatively narrow (approximately 1.2–1.5). In the case of **$P_{45}M_{200}$**, the GPC measurement was carried out using $NaNO_3$ aq. (100 mM) as an eluent, because of low solubility in DMF solution. The M_n was larger than the expectation, which indicate the part of polymer was aggregated in aqueous solution. These results

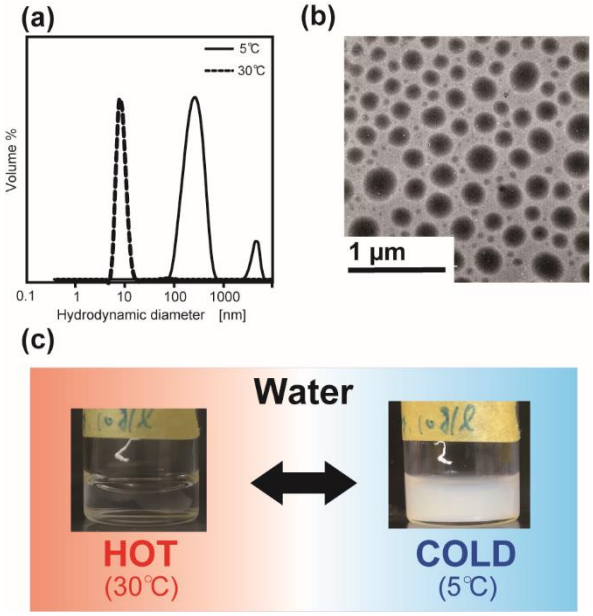

Figure 1 (a) the DLS result of $P_{45}M_{200}$ at 5 and 30°C. (b) TEM observation of $P_{45}M_{200}$ stained by Osmium Tetroxide. (c) the temperature dependence on the turbidity of the $P_{45}M_{200}$ aqueous solution.

demonstrated that the DHBGs had been successfully synthesized.

3-2. Self-assembly capability of the DHBGs

3-2-1. Self-assembly capability of $P_{45}M_{200}$ as a representative

As a representative, the self-assembly capability of **$P_{45}M_{200}$** was investigated by DLS and TEM. The polymer was dissolved in HEPES buffer (polymer concentration: 10 g L^{-1}). DLS revealed that **$P_{45}M_{200}$** had scattering with narrow volume distribution at 5°C; the average hydrodynamic diameter of the resulting structure was approximately 330 ± 50 nm at 5°C (Fig. 1 (a)). However, part of the polymer was precipitated, and formed a membrane structure (Fig. S29). The structure was confirmed by TEM and the average size was determined to be 177 ± 74 nm (Fig. 1 (b)). Furthermore, the polymer solution became turbid at low temperatures (approximately 5°C), and transparent at high temperatures (above 30°C) (Fig. 1 (c)).

These results indicate that **$P_{45}M_{200}$** self-assembled in aqueous solution. Moreover, it has been reported that polymers with hydrogen bonding capability in solution become transparent at high temperatures and turbid at low temperatures.[18,20] Therefore, the change in the scattering of the DHBG and apparent turbidity revealed by the DLS measurements suggest that this system exhibited upper critical solution temperature (UCST) behavior due to hydrogen bonding.

3-2-2. Self-assembly of the mannose homopolymer

In the presence of guanidine hydrochloride, an aqueous solution of the mannose homopolymer (**M_{200}**) was transparent, and the absorbance at 500 nm was 0.01 after incubation for 23 h at 5°C. However, an aqueous solution of **M_{200}** with sodium chloride instead of guanidine hydrochloride was turbid after incubation for 23 h at 5°C, and the absorbance at 500 nm was 0.39 ± 0.17 (Fig. 2). The transmittance values with and without guanidine hydrochloride were 96.8 and 40.6%, respectively.

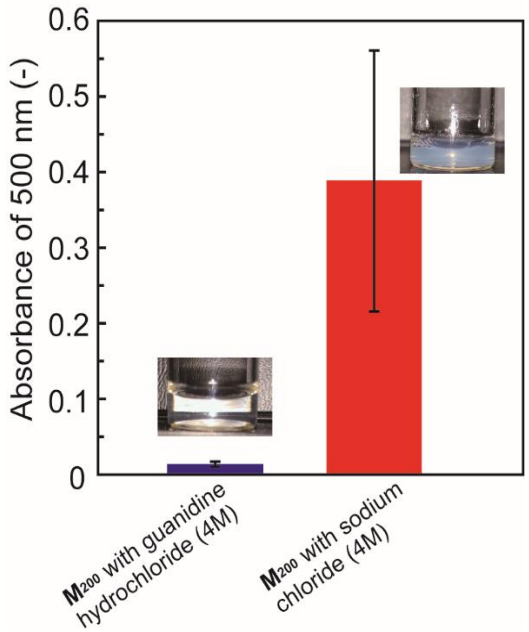

Figure 2 The turbidity measurement of M_{200} aqueous solution with guanidine hydrochloride (blue) and with sodium chloride instead of guanidine hydrochloride (red).

Guanidine hydrochloride is used to cleave hydrogen bonds. Therefore, the results indicate that the guanidine hydrochloride cleaved the hydrogen bonds in the glycopolymer, making the polymer solution transparent. The results reveal that there were hydrogen bonding interactions in the glycopolymer. Mannose contains numerous hydroxy groups per unit volume, which indicates that it is possible to create hydrogen bonds between glycopolymers. Abeyratne-Perera *et al.* reported that the surface of mannose exhibits self-latching behavior via strong hydrogen bonding.[21] The results indicate that DHBGs composed of glycopolymer and PEG self-assemble in aqueous solution owing to the hydrogen bonding between the glycopolymer moieties. The glycopolymer moieties seemed to be located in the interior of the molecular assembly of $\mathbf{P_{45}M_{200}}$. However, the interaction with each PEG unit did not exceed that with the glycopolymer moieties[18]. No interactions between glycopolymer moieties and PEG were observed.[18] Therefore, DHBGs comprise a glycopolymer interior and a PEG exterior.

3-2-3. The self-assembly of DHBGs

The other DHBG variants were studied by DLS and TEM. The average hydrodynamic diameter of $\mathbf{P_{45}M_{100}}$, $\mathbf{P_{45}M_{200}}$, $\mathbf{P_{90}M_{100}}$, and $\mathbf{P_{90}M_{200}}$ at 5°C were 180 ± 50, 330 ± 50, 40 ± 3, and 90±5 nm, respectively. (Table 3 and Fig. S22-S24). $\mathbf{P_9M_{100}}$, $\mathbf{P_9M_{200}}$, and part of $\mathbf{P_{45}M_{200}}$ formed membrane structures after incubation overnight at 5°C owing to low dispersibility (Fig. S29). In contrast, $\mathbf{P_{90}M_{200}}$ readily formed and maintained a self-assembled structure, and did not form a membrane structure after incubation at 5°C, even though it had the same glycopolymer length as $\mathbf{P_9M_{200}}$ and $\mathbf{P_{45}M_{200}}$. The DHBGs with shorter glycopolymers ($\mathbf{M_{10}}$) exhibited scattering at less than 10 nm, and such polymer solutions are transparent. DHBGs with short PEG chains ($\mathbf{P_9}$) were also less likely to self-assemble. The average sizes of $\mathbf{P_9M_{200}}$, $\mathbf{P_{45}M_{100}}$, $\mathbf{P_{45}M_{200}}$, $\mathbf{P_{90}M_{100}}$, and $\mathbf{P_{90}M_{200}}$ were determined by TEM to be 173 ± 19, 72 ± 30, 177 ± 74, 31 ± 5, and 56 ± 9 nm, respectively (Fig. S26). According to the TEM observations, these DHBGs self-assembled into apparent spherical structure structures in dry state, regardless of the ratio of PEG to glycopolymer.

Table 3 The self-assembly of each DHBG(-: no-assembly, *DLS measurement was carried out at 5°C without incubation).

		DP of glycopolymer		
		10	**100**	**200**
DP of PEG	**9**	-	-	1500± 350* nm
	45	-	180 ± 50 nm	330 ± 50 nm
	90	-	40 ± 3 nm	90±5 nm

Three of the DHBGs—i.e., $\mathbf{P_{45}M_{100}}$, $\mathbf{P_{90}M_{100}}$, and $\mathbf{P_{90}M_{200}}$—self-assembled to form apparent spherical structure (Fig. S26). $\mathbf{P_9M_{200}}$ and $\mathbf{P_9M_{100}}$ formed insoluble membrane structures after incubation at 5°C. The other polymers did not self-assemble in the aqueous solution owing to the water solubility of the polymers. Amphiphilic block copolymers self-assemble into various structures, such as micelles, worms, and vesicles, depending on the block polymer ratio. In the present investigation of DHBGs with various block ratios, the polymers only self-assembled into the same structures. These data show a difference in self-assembly behavior between the DHBGs and amphiphilic block copolymers. The components of DHBGs are hydrophilic and do not repel water like the hydrophobic segments of amphiphilic polymers. It is possible that the PEG moieties exist at the periphery of the glycopolymer core, but do not perfectly cover all of it. DHBGs have an inhomogeneous and spherical structure. The self-assembly of DHBGs is mainly induced by hydrogen bonding between glycopolymer moieties. The DHBGs with a shorter glycopolymer ($\mathbf{M_{10}}$) did not self-assemble. The DHBGs with a longer glycopolymer moiety ($\mathbf{M_{100}}$, $\mathbf{M_{200}}$) were more likely to self-assemble, and three of the DHBGs ($\mathbf{P_9M_{100}}$, $\mathbf{P_9M_{200}}$, and part of $\mathbf{P_{45}M_{200}}$) formed membrane structures owing to strong molecular interactions. Furthermore, the block copolymer structure is essential for this regular spherical structure.[9,18]

3-2-4 The effect of PEG length on the UCST behavior

The self-assembly capabilities of $\mathbf{P_9M_{200}}$, $\mathbf{P_{45}M_{200}}$, and $\mathbf{P_{90}M_{200}}$ were compared by temperature swing DLS (Fig. 3). The hydrodynamic diameter of the polymers between 40 and 20°C in cooling process calculated from the scattering were less than 10 nm. The hydrodynamic diameter increased below 20°C. When the polymer solution was heated up from 5°C, the hydrodynamic diameter increased, although the hydrodynamic diameter were initially less than 10 nm (Fig. S28). $\mathbf{P_9M_{200}}$ formed a homogeneous aqueous solution between 40 and 20°C in cooling process, and produced considerable scattering at low temperatures (below 20°C), but failed to re-dissolve as the

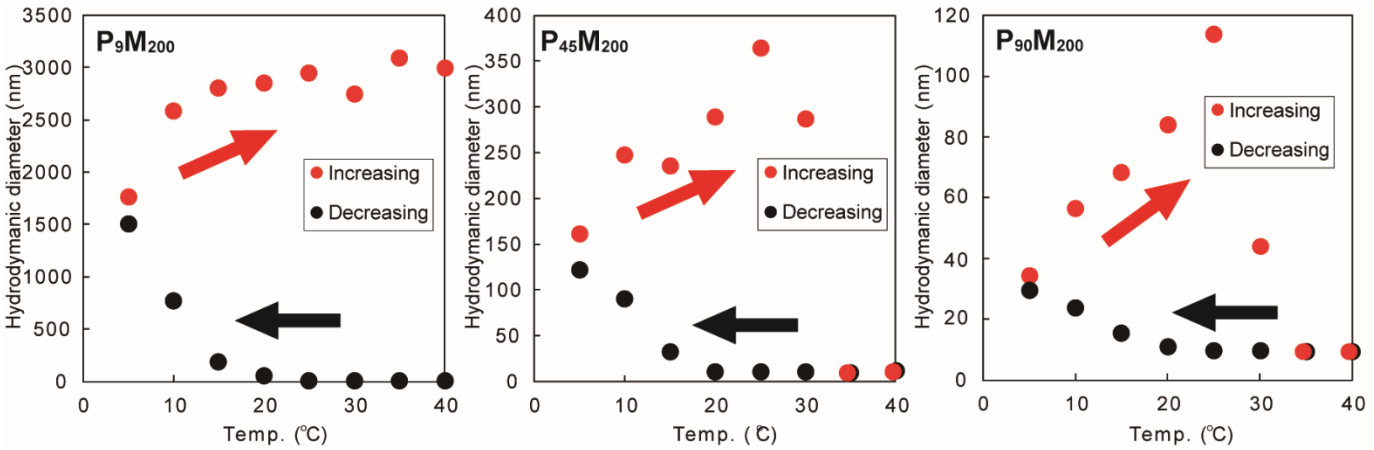

Figure 3 The temperature dependence of hydrodynamic diameter of P_9M_{200}, $P_{45}M_{100}$ and $P_{90}M_{200}$ (black: decreasing temperature process, red: increasing temperature process), Schematic illustration of the effect of PEG length on the P_mM_{90} (m: 9, 45, 90) self-assembly.

temperature increased. Moreover, the hydrodynamic diameter of the DHBGs decreased with decreasing PEG length.

DHBGs with similar glycopolymer lengths started to self-assemble at approximately the same temperature (20°C for DHBG with $\mathbf{M_{200}}$). The hydrodynamic diameter was influenced by the PEG length. The longer the PEG length, the smaller and more stable the self-assembled structure obtained. It is thought that PEG inhibits the aggregation of the glycopolymer moiety via steric hindrance, producing a small self-assembled structure. Moreover, self-assembly was dissociated in $\mathbf{P_{45}M_{200}}$ and $\mathbf{P_{90}M_{200}}$ at temperatures above 30°C. This phenomenon also indicated that such self-assembly exhibits UCST behavior. The self-assembly of DHBGs arises from supramolecular interactions. In the case of the glycopolymer, hydrogen bonding formation is the main driving force. Several polymers with functional hydrogen-binding groups have demonstrated UCST behavior[20]. The DHBGs in the present study exhibited similar functionality to such polymers.

Moreover, the hydrodynamic diameter increased as the polymers were heated from 5 to 30°C. The DHBGs begin to self-assemble into small structure below 20°C owing to hydrogen bonding. At such low temperatures, the glycopolymer moieties aggregate to form a glycopolymer core, with PEG supposedly forming the exterior of the self-assembly. Unlike amphiphilic block copolymer, the interacting polymer which is glycopolymer are not completely coated with PEG. Therefore, the primary self-assembly can also interact with each other via hydrogen bonding, leading to an increase in size (Fig. S28). Especially in heating process, the entropy of primary self-assembly become large, which leads to promote the interaction between the self-assembly. Thus, the dynamic self-assembly of DHBGs depends on various factors such as temperature and concentration.
The conclusions section should come in this section at the end of the article, before the acknowledgements.

3-2-5 The effect of incubation time on the size of the self-assembled structures

The hydrodynamic diameter of each polymer at 5°C from the temperature swing according to DLS was much smaller than the DLS result at 5°C after overnight incubation. The hydrodynamic diameter increased gradually as the polymer solution was incubated at 5°C. This indicates that the self-assembly size was not only affected by the temperature, but also by the incubation time. This result also suggests that the PEG moiety of DHBG was unable to coat the glycopolymer core fully, and that it is possible for the glycopolymer cores to fuse with each other to form a larger self-assembled structure. Therefore, the DHBGs initially self-assembled into small structures, and then formed pseudo-equilibrium self-assembled structures. We propose that these DHBGs self-assembled as a result of hydrogen bonding with UCST behavior, and their size increased owing to their mobility. The DHBGs also exhibited dynamic properties.

3-2-6 The effect of polymer concentration on self-assembly

The concentration dependence of the hydrodynamic diameter of $\mathbf{P_9M_{200}}$, $\mathbf{P_{45}M_{100}}$, $\mathbf{P_{45}M_{200}}$, $\mathbf{P_{90}M_{100}}$, and $\mathbf{P_{90}M_{200}}$ was evaluated by DLS. The hydrodynamic diameter of the self-assembled structures at polymer concentrations of 1 and 10 g L^{-1} were compared (Fig. 4). The hydrodynamic diameter of $\mathbf{P_9M_{200}}$, $\mathbf{P_{45}M_{100}}$, $\mathbf{P_{45}M_{200}}$, $\mathbf{P_{90}M_{100}}$, and $\mathbf{P_{90}M_{200}}$ at 1 g L^{-1} after incubation at 5°C were 1110 ± 270, 60 ± 2, 110 ± 6, 60 ± 5, and 70 ± 2 nm, respectively (Fig. S25). The self-assembled structures of $\mathbf{P_9M_{200}}$, $\mathbf{P_{45}M_{200}}$, and $\mathbf{P_{45}M_{100}}$ at 1 g L^{-1} were smaller than those at 10 g L^{-1}, whereas $\mathbf{P_{90}M_{100}}$ and $\mathbf{P_{90}M_{200}}$ had almost the same hydrodynamic diameter at the two concentrations.
In $\mathbf{P_9M_{200}}$, $\mathbf{P_{45}M_{200}}$, and $\mathbf{P_{45}M_{100}}$, the lower concentration reduced the chance of fusion between the self-assembled structures, resulting in smaller hydrodynamic diameter. This result indicates that large self-assembled structures are formed by the collision and fusion of smaller PEG-deficient structures. However, in $\mathbf{P_{90}M_{100}}$ and $\mathbf{P_{90}M_{200}}$ the self-assembly size did not depend on concentration because the PEG length was sufficient to prevent fusion between the polymers.

It is thought that the self-assembly process of DHBG comprises two stage. DHBG self-assembles into small structures with a low association number in the initial stage. The PEG density of the structure is low in this state, because of the low

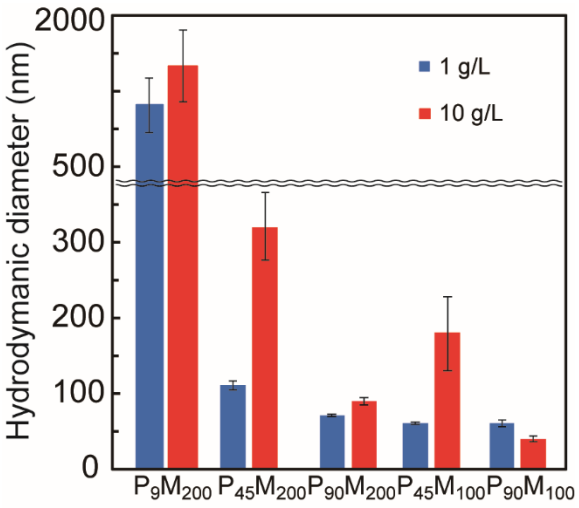

Figure 5 The polymer concentration dependence of the DHBG's self-assembly.

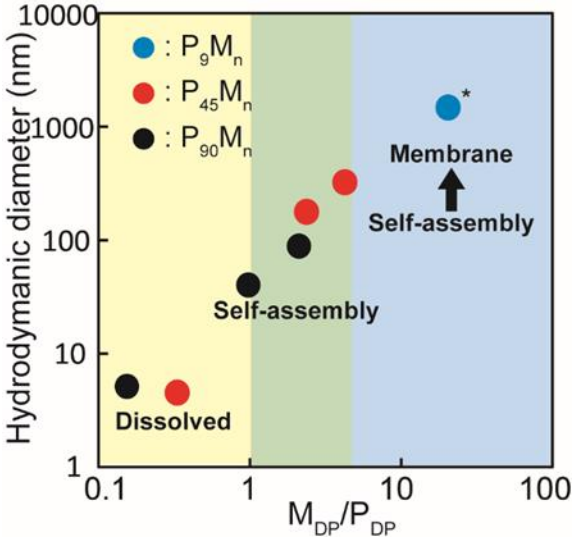

Figure 4 The DLS result with polymer concentration at 10 g/L after incubation at 5°C for 1 day. * DLS measurement was carried out at 5°C without incubation (Fig.3).

association number. Therefore, the glycopolymer cores are easily exposed to the exterior and readily fuse with each other. Once DHBGs self-assemble into small structures, their size increases owing to collision and fusion of the glycopolymer to form a pseudo-equilibrium self-assembled structure. The size of the pseudo-equilibrium self-assembled structure depends on the PEG length. When the PEG is short, a greater association number is required to prevent glycopolymer fusion, which results in a larger structure. The results suggest that self-assembly and stability depend on the block polymer ratio of the DHBGs. The self-assembled DHBG structure is not unambiguous like that of amphiphilic molecules, but is strongly dependent on the block polymer ratio.

3-2-7 The effect of the ratio of glycopolymer to PEG length on self-assembly

To investigate the effect of the ratio of glycopolymer to PEG length on pseudo-equilibrium self-assembly, the hydrodynamic diameter of each DHBG (polymer concentration: 10 g/L) after incubation at 5°C was plotted against the ratio of glycopolymer to PEG length (M_{DP}/P_{DP}), as shown in Fig. 5. Interestingly, Fig. 5 shows that the self-assembly property of DHBG can be classified according to the M_{DP}/P_{DP} ratio. When the M_{DP}/P_{DP} was between 0.1 and 1, the DHBG did not self-assemble, but dissolved as one molecule in the water (Fig. 5, yellow state). However, the DHBGs with M_{DP}/P_{DP} ratios between 1 and 10 self-assembled into the structures (Fig. 5, green state). Initially, the DHBGs with M_{DP}/P_{DP} ratios over 10 self-assembled into the structures, but ultimately formed membrane structures (Fig. 5, blue state). The hydrodynamic diameter increased with increasing M_{DP}/P_{DP}, despite the differences in the length of the polymer as a whole. When the DPs of the PEG were 45 and 90, the hydrodynamic diameter of the self-assembled structures increased in proportion to the DP of the Man-MA (sugar unit). When the DP of the Man-MA of the glycopolymer was held constant, the hydrodynamic diameter was inversely proportional to the DP of the PEG. As the association number of the self-assembly increased, the density of the PEG located on the exterior increased. Therefore, DHBGs with short PEGs have greater association numbers and form large particles until the PEG density inhibits fusion via particle collision. Furthermore, when the PEG length is insufficient to inhibit fusion, the DHBG forms a membrane structure. No morphological changes took place in the DHBG block polymer, unlike during the self-assembly of amphiphilic polymers. However, there seems to be a correlation between the ratio of the block polymer and the size of the self-assembled structure. It may be possible to control the size of the self-assembled structure by adjusting the block polymer ratio.

Conclusions

DHBG composed of PEG and glycopolymer with mannose side chains self-assembles in aqueous solution and exhibits UCST behavior. The driving force behind the self-assembly is hydrogen bonding of the mannose side chain, and the self-assembled structure grows in size and stability from 5 to 30°C. The size of the self-assembled structure is dependent on the ratio of PEG to glycopolymer length. Unlike self-assembled amphiphilic block copolymers, DHBG self-assembled structures are the same structure in all cases. Furthermore, the PEG length has a strong influence on dispersibility. When the PEG length is insufficient to coat the glycopolymer core, the self-assembled structures fuse to form a large self-assembled structure and a membrane structure. The dynamic self-assembly of DHBGs is affected by temperature, polymer concentration, and incubation time. Specially, the UCST behavior of the DHBGs is an important aspect of self-assembly. Our results provide a guideline for understanding and directing DHBG self-assembly, which we hope will expand the application of double hydrophilic block copolymer self-assembly chemistry. This novel type of material could be used to compartmentalize water-soluble substances within the aqueous phase.

Conflicts of interest

The authors declare no conflict of interest.

Acknowledgements

This work was supported by a JSPS KAKENHI Grant Number JP20H05230, JP20H04825, JP19K22971 and JP19H02766.

Notes and references

1 J. W. Szostak, D. P. Bartel and P. L. Luisi, *Nature*, 2001, **409**, 387–390.

2 P. Tanner, P. Baumann, R. Enea, O. Onaca, C. Palivan and W. Meier, *Acc. Chem. Res.*, 2011, **44**, 1039–1049.

3 S. Sugihara, A. Blanazs, S. P. Armes, A. J. Ryan and A. L. Lewis, *J. Am. Chem. Soc.*, 2011, **133**, 15707–15713.

4 A. Blanazs, J. Madsen, G. Battaglia, A. J. Ryan and S. P. Armes, *J. Am. Chem. Soc.*, 2011, **133**, 16581–16587.

5 P. Tanner, P. Baumann, R. Enea, O. Onaca, C. Palivan and W. Meier, *Acc. Chem. Res.*, 2011, **44**, 1039–1049.

6 G. Delaittre, I. C. Reynhout, J. J. L. M. Cornelissen and R. J. M. Nolte, *Chem. - A Eur. J.*, 2009, **15**, 12600–12603.

7 K. H. Markiewicz, L. Seiler, I. Misztalewska, K. Winkler, S. Harrisson, A. Z. Wilczewska, M. Destarac and J.-D. Marty, *Polym. Chem.*, 2016, **7**, 6391–6399.

8 C. Frangville, Y. Li, C. Billotey, D. R. Talham, J. Taleb, P. Roux, J. D. Marty and C. Mingotaud, *Nano Lett.*, 2016, **16**, 4069–4073.

9 S. M. Brosnan, H. Schlaad and M. Antonietti, *Angew. Chemie - Int. Ed.*, 2015, **54**, 9715–9718.

10 A. Blanazs, N. J. Warren, A. L. Lewis, S. P. Armes and A. J. Ryan, *Soft Matter*, 2011, **7**, 6399–6403.

11 G. Pasparakis and C. Alexander, *Angew. Chemie - Int. Ed.*, 2008, **47**, 4847–4850.

12 A. Harada and K. Kataoka, *Science (80-.).*, 1999, **283**, 65–67.

13 A. Harada and K. Kataoka, *Macromolecules*, 1995, **28**, 5294–5299.

14 B. V. K. J. Schmidt, *Macromol. Chem. Phys.*, 2018, **219**, 1–15.

15 N. Al Nakeeb, J. Willersinn and B. V. K. J. Schmidt, *Biomacromolecules*, 2017, **18**, 3695–3705.

16 A. Plucinski, J. Willersinn, R. B. Lira, R. Dimova and B. V. K. J. Schmidt, *Macromol. Chem. Phys.*, 2020, **221**, 2000053–2000063.

17 A. Koide, A. Kishimura, K. Osada, W. D. Jang, Y. Yamasaki and K. Kataoka, *J. Am. Chem. Soc.*, 2006, **128**, 5988–5989.

18 T. Oh, M. Nagao, Y. Hoshino and Y. Miura, *Langmuir*, 2018, **34**, 8591–8598.

19 J. Quan, F. W. Shen, H. Cai, Y. N. Zhang and H. Wu, *Langmuir*, 2018, **34**, 10721–10731.

20 N. Shimada, H. Ino, K. Maie, M. Nakayama, A. Kano and A. Maruyama, *Biomacromolecules*, 2011, **12**, 3418–3422.

21 H. K. Abeyratne-Perera and P. L. Chandran, *Langmuir*, 2017, **33**, 9178–9189.